Electronic Supplementary Material (ESI) for New Journal of Chemistry.

Ni modified CuS-based self-supported electrocatalyst with nanobeads-like porous morphology for efficient hydrogen production in basic media.

Vishal V. Burungale[1], Hyojung Bae[2], Pratik Mane[1], An-Na Cha[3], Sang-Wan Ryu[2], Soon-Hyung Kang[2], Jun-Seok Ha[1,2,3]*

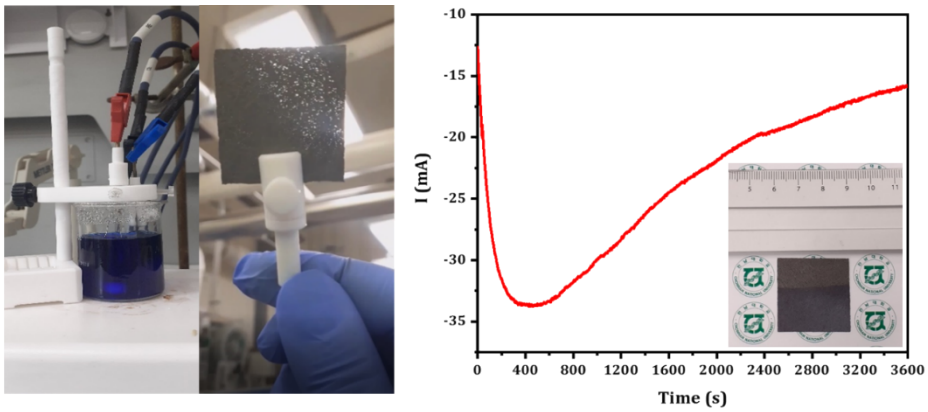

Before deposition (g)	After deposition (g)	Weight difference (g)	Area of Substrate (cm^2)	Mass per cm^2 of substrate (g/cm^2)	Area of deposition (cm^2)	Catalyst loading (g/cm^2)
0.1259	0.1919	0.0660	8.980	0.014020	5.582	0.011824

Figure S1 The photographs of the actual experimental setup, the graph of Current vs Time during electrodeposition, and details of catalyst loading of the CFP_C sample.

Sample Name	Area (cm^2)
CFP	0.794
CFP_C	0.951
CFP_CCS	0.828
CFP_CSN	0.817

Figure S2 The photographs of actual samples used for electrochemical study and tables containing details of measured sample areas.

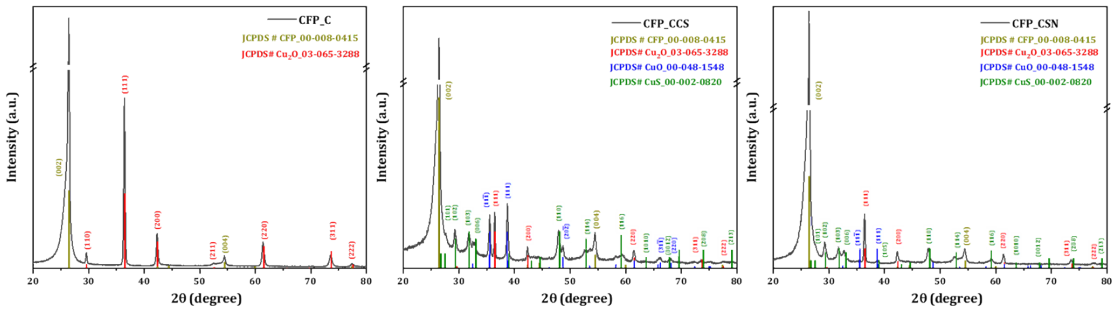

Figure S3 The XRD patterns of CFP_C, CFP_CCS, and CFP_CSN samples with their respective standard XRD patterns.

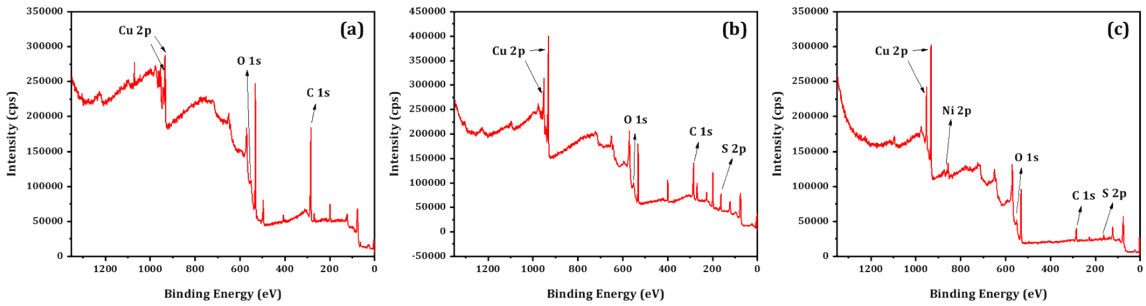

Figure S4 XPS Survey spectra of CFP_C, CFP_CCS, and CFP_CSN samples.

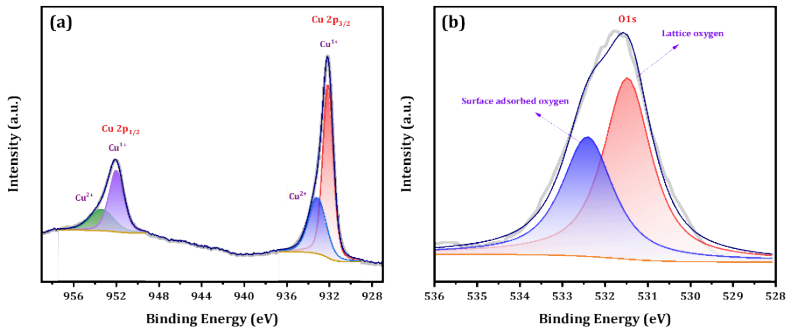

Figure S5 Narrow scan XPS spectra of (a) Cu, (b) O, for CFP_C sample

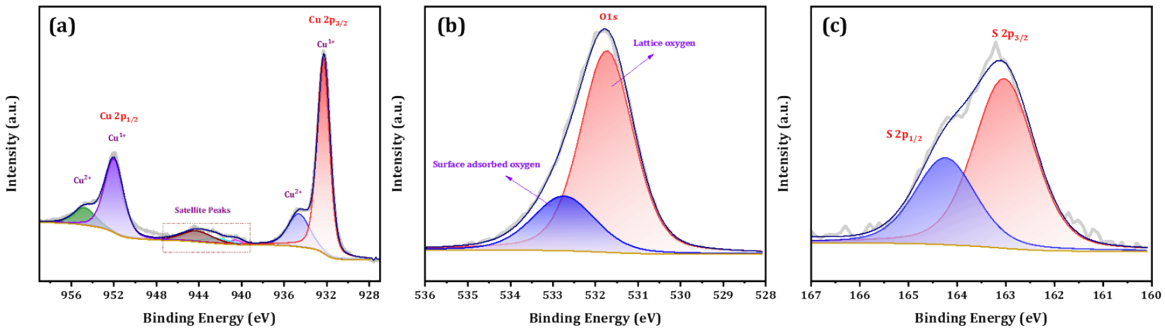

Figure S6 Narrow scan XPS spectra of (a) Cu, (b) O, (c) S for CFP_CCS sample

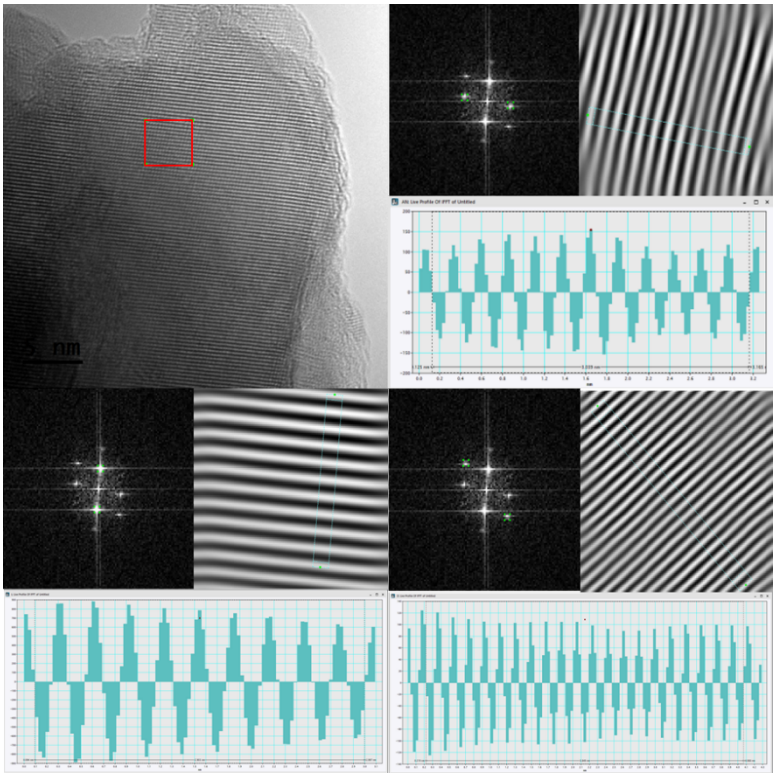

Figure S7 The images related to measurement of interplanar distance using Gatan Software

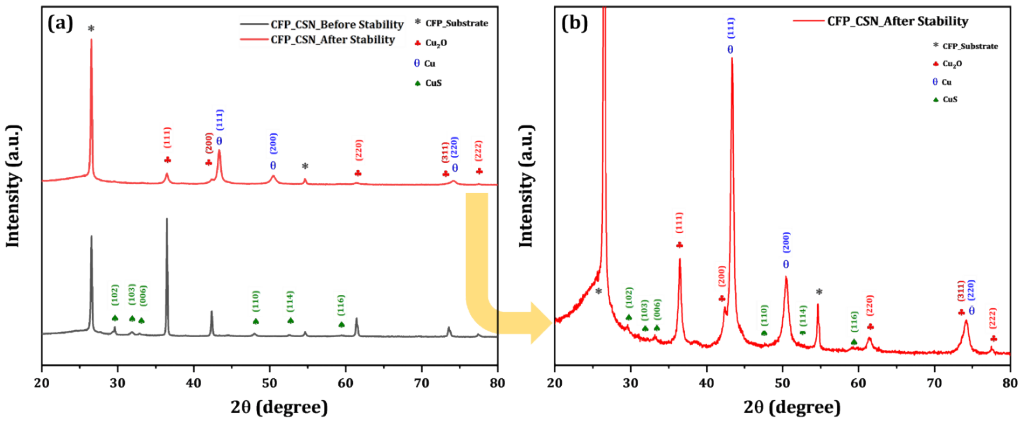

Figure S8 (a) XRD patterns of CFP_CSN sample before and after stability, (b) Enlarged version of after stability XRD pattern to show small peaks related to CuS.

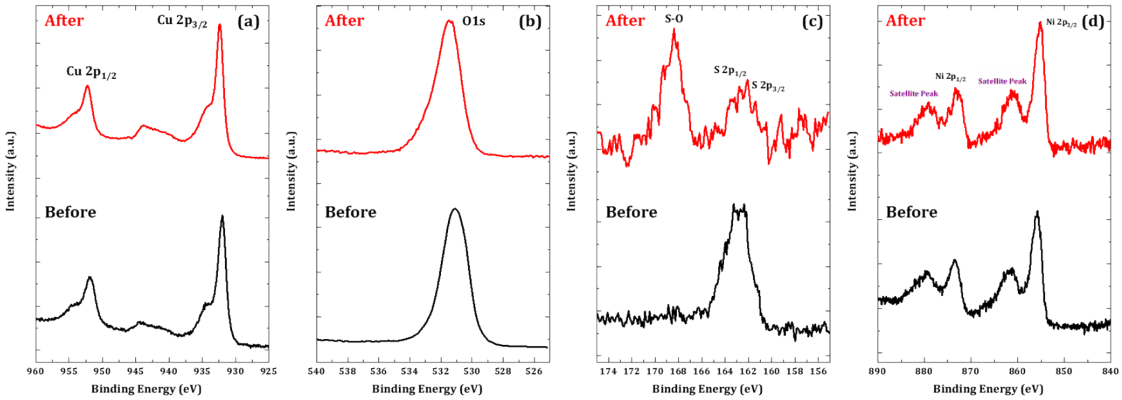

Figure S9 The comparative XPS narrow scan spectrums of (a) Cu, (b) O, (c) S, and (d) Ni before and after the stability experiment.

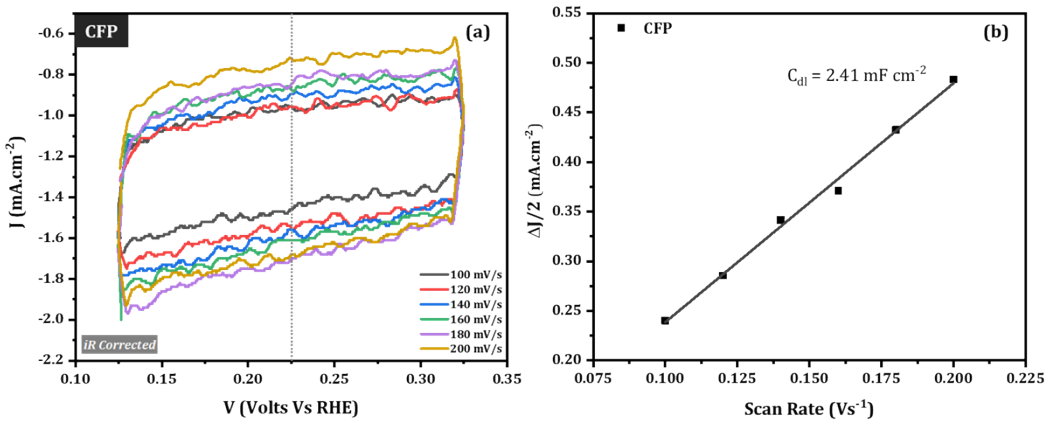

Figure S10 (a) Cyclic Voltammetry curves measured in a non-Faradaic region of CFP samples at different scan rates and (b) Corresponding Linear regression between current density differences in the middle of the potential window of CV vs. Scan Rates.

Table S1 The details of catalyst loading of sulfurized samples measured by the weight difference method.

	Area of Substrate (cm^2)	Calculated mass of substrate (g)	Before Sulfurization (g)	After Sulfurization (g)	Weight difference (g)	Actual mass of catalyst (g)	Area of deposition (cm^2)	Catalyst loading (g/cm^2)
Without Ni	1.462	0.0205	0.0316	0.0297	-0.0019	0.0092	0.876	0.010502
With Ni	1.491	0.0209	0.0331	0.0306	-0.0025	0.0097	0.866	0.011201

Table S2. EIS equivalent circuit fitting data

	R_u ($\Omega.cm^2$)	Y_0	n	R_{CT} ($\Omega.cm^2$)
CFP	1.426	0.00026	0.8589	282.90
CFP_C	1.202	0.02796	0.8273	6.12
CFP_CCS	1.162	0.05352	0.8603	2.60
CFP_CSN	1.021	0.06764	0.8346	0.76

Table S3. Comparison of HER activity with some of the previously reported Cu based electrocatalysts.

Catalyst	Substrate	Tafel Slope (mV/dec)	Electrolyte	Current density (mA/cm^2)	Overpotential (mV)	Reference
Alkaline electrolyte						
$Cu_2O/CuS/Ni$	CFP	91.54	1.0 M KOH	10	216	This work
				50	285	
				100	325	
CuS	GCE	244	1.0 M KOH	10	447	[1]
Cu_2O/CuS	GCE	212	1.0 M KOH	10	240	[1]
Cu_2O-200	GCE	106	1.0 M KOH	10	184	[2]
$CuFe_{0.6}S_{1.6}$	CFP	101	1.0 M KOH	10	237	[3]
CuO@UiO-66	NF	164	2.0 M KOH	10	220	[4]
Cu/Cu-MOF/GO	CF	201	1.0 M KOH	10	250	[5]
$Ni_9S_8/CuS/Cu_2O/NF$	NF	163	1.0 M KOH (0.33 M Urea)	10	146	[6]
Neutral Electrolyte						
Y-Cu_2S	CF	98.9	1 M KPi	10	190	[7]
Acidic Electrolyte						
Cu-C_3N4	GCE	~76	0.5M H_2SO_4	10	390	[8]
CuS	GCE	171	0.5M H_2SO_4	10	449	[9]

CuS-Au	GCE	75	0.5M H_2SO_4	10	179	[9]
Ag_2S/CuS	GCE	75	0.5M H_2SO_4	10	193	[10]
CuS/MoS_2	GCE	80	0.5M H_2SO_4	10	225	[11]
0.1rGO-CuS	GCE	61	0.5M H_2SO_4	10	179	[12]
MoS_2/CuS	GCE	63	0.5M H_2SO_4	10	290	[13]
CuS	CFP	144	0.5M H_2SO_4	10	449	[14]
CuO-NiO/CN	GP	171	0.5M H_2SO_4	10	762	[15]

References:

1. S.-Q. Liu, H.-R. Wen, G. Ying, Y.-W. Zhu, X.-Z. Fu, R. Sun and C.-P. Wong, *Nano Energy*, 2018, **44**, 7-14.
2. M. Wang, X. Cheng and Y. Ni, *Dalton Trans*, 2019, **48**, 823-832.
3. X. Li, N. Ye, H. Liu, C. Li, Y. Huang, X. Zhu, H. Feng, J. Lin, L. Huang, J. Wu, Y. Liu, C. Liang and X. Peng, *International Journal of Hydrogen Energy*, 2022, **47**, 16719-16728.
4. M. Fiaz, M. Athar, S. Rani, M. Najam-ul-Haq and M. A. Farid, *Materials Chemistry and Physics*, 2020, **239**.
5. L. Ye and Z. Wen, *Chem Commun (Camb)*, 2018, **54**, 6388-6391.
6. D. Wei, W. Tang and Y. Wang, *International Journal of Hydrogen Energy*, 2021, **46**, 20950-20960.
7. M. Fan, R. Gao, Y.-C. Zou, D. Wang, N. Bai, G.-D. Li and X. Zou, *Electrochimica Acta*, 2016, **215**, 366-373.
8. X. Zou, R. Silva, A. Goswami and T. Asefa, *Applied Surface Science*, 2015, **357**, 221-228.
9. M. Basu, R. Nazir, P. Fageria and S. Pande, *Sci Rep*, 2016, **6**, 34738.
10. H. Ren, W. Xu, S. Zhu, Z. Cui, X. Yang and A. Inoue, *Electrochimica Acta*, 2016, **190**, 221-228.
11. A. Bar-Hen, R. Bar-Ziv, T. Ohaion-Raz, A. Mizrahi, S. Hettler, R. Arenal and M. Bar Sadan, *Chemical Engineering Journal*, 2021, **420**.
12. H. Wang, L. Hu, H. Zhou and Y. Zhang, *International Journal of Hydrogen Energy*, 2021, **46**, 35239-35247.
13. L. Zhang, Y. Guo, A. Iqbal, B. Li, D. Gong, W. Liu, K. Iqbal, W. Liu and W. Qin, *International Journal of Hydrogen Energy*, 2018, **43**, 1251-1260.
14. L. An, L. Huang, P. Zhou, J. Yin, H. Liu and P. Xi, *Advanced Functional Materials*, 2015, **25**, 6814-6822.
15. S. B. Khan and A. M. Asiri, *Journal of Molecular Liquids*, 2021, **335**.